

A grid of synthetic spectra and indices Fe5270, Fe5335, Mgb and Mg₂ as a function of stellar parameters and $[\alpha/\text{Fe}]$ ^{★,★★}

B. Barbuy¹, M.-N. Perrin², D. Katz³, P. Coelho¹, R. Cayrel², M. Spite³, and C. Van 't Veer-Menneret³

¹ Universidade de São Paulo, Rua do Matão 1226, São Paulo 05508-900, Brazil
e-mail: pcoelho@usp.br

² Observatoire de Paris, 61 av. de l'Observatoire, 75014 Paris, France
e-mail: Marie-Noel.Perrin@obspm.fr, Roger.Cayrel@obspm.fr

³ Observatoire de Paris-Meudon, 92195 Meudon, France
e-mail: David.Katz@obspm.fr, Monique.Spite@obspm.fr, Claude.Vantveer@obspm.fr

Received 30 August 2000 / Accepted 20 March 2003

Abstract. We have computed a grid of synthetic spectra in the wavelength range $\lambda\lambda$ 4600–5600 Å using revised model atmospheres, for a range of atmospheric parameters and values of $[\alpha\text{-elements}/\text{Fe}] = 0.0$ and $+0.4$. The Lick indices Fe5270, Fe5335, Mgb and Mg₂ are measured on the grid spectra for $FWHM = 2$ to 8.3 Å. Relations between the indices Fe5270, Fe5335 and Mg₂ and the stellar parameters effective temperature T_{eff} , $\log g$, $[\text{Fe}/\text{H}]$ and $[\alpha/\text{Fe}]$, valid in the range $4000 \leq T_{\text{eff}} \leq 7000$ K, are presented. These fitting functions are given for $FWHM = 3.5$ and 8.3 Å. The indices were also measured for a list of 97 reference stars with well-known stellar parameters observed at ESO and OHP, and these are compared to the computed indices. Finally, a comparison of the indices measured on the observed spectra and those derived from the fitting functions based on synthetic spectra is presented.

Key words. stars: abundances

1. Introduction

Libraries of stellar spectra for a range of atmospheric parameters are a useful tool for the study of stellar populations. In the literature libraries of spectra both observed and synthetic (e.g. Allard & Hauschildt 1995; Gunn & Stryker 1983; Jacoby et al. 1984; Kurucz 1993; Lejeune et al. 1997, 1998; Soubiran et al. 1998; Schiavon & Barbuy 1999) are used in calculations of population synthesis (e.g. Bruzual & Charlot 1993, 2003). Spectral indices, among which the most used are the Lick Fe5270 and Fe5335, Mgb and Mg₂ ones (Burstein et al. 1984; Faber et al. 1985; Worthey et al. 1994), are also of great interest in studies of composite systems (e.g. Gorgas et al. 1993; Worthey 1994; Worthey et al. 1994).

Indices derived from the computation of synthetic spectra were presented by Gulati et al. (1993), where the ATLAS code, line lists and model atmospheres by Kurucz (1993) were employed; Barbuy (1994) computed Mg₂ for representative stellar

evolutionary stages of globular clusters, for metallicities in the range $-2.0 < [\text{Fe}/\text{H}] < +0.5$, and composite spectra for single-aged populations, deriving a calibration of Mg₂ vs. $[\text{Fe}/\text{H}]$ and $[\text{Mg}/\text{Fe}]$. Tripicco & Bell (1995, hereafter TB95) computed a series of 21 Lick indices, taking into account changes in the abundances of individual elements. For each of the elements C, N, O, Mg, Fe, Ca, Na, Si, Cr and Ti, calculations with different abundance values were carried out, and effects of the abundance changes of each of these particular elements on the different indices were measured.

In the present work we compute synthetic spectra, using revised lists of atomic and molecular data and revised model atmospheres, thus improving the grid of synthetic spectra as used by Cayrel et al. (1991). The Fe5270, Fe5335, Mgb and Mg₂ indices are measured on the grid spectra, convolved with Gaussians of $FWHM = 2.0$ to 8.3 Å. A comparison between the synthetic indices and those measured on a sample of reference stars are presented. Our intent is to reveal the effects caused on the indices by changes in the abundances of all the α -elements at the same time, therefore in this respect a different approach relative to that by TB95. Finally, fitting functions of the indices Fe5270, Fe5335 and Mg₂ measured on synthetic spectra, convolved with $FWHM = 3.5$ and 8.3 Å, are presented.

In Sect. 2 the theoretical grid is described. In Sect. 3 the theoretical indices are reported, and their behaviour with respect

Send offprint requests to: B. Barbuy,
e-mail: barbuy@astro.iag.usp.br

* Observations collected at the European Southern Observatory (ESO), La Silla, Chile and at the Observatoire de Haute Provence (OHP), St-Michel, France.

** All Tables of Appendices A and B are only available in electronic form at the CDS via anonymous ftp to cdsarc.u-strasbg.fr (130.79.128.5) or via
<http://cdsweb.u-strasbg.fr/cgi-bin/qcat?A+A/404/661>

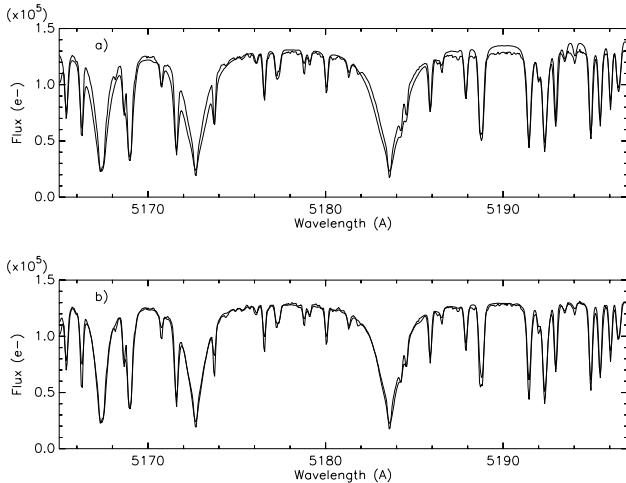


Fig. 1. Solar spectrum observed (thick lines) at a resolution of $R = 42\,000$ with the ELODIE spectrograph compared to synthetic spectra (thin lines) computed with revised ATLAS9 models (Sect. 2.1). Damping constants and oscillator strengths were obtained from a fit to the solar spectrum employing **a)** the HM74 model; **b)** ATLAS9 solar atmospheric model computed in this work, for which the atomic constants were fitted.

to stellar parameters is studied. In Sect. 4 the observed spectra and corresponding indices are reported. A summary is given in Sect. 5. In Appendix A the fitting functions coefficients are presented. In Appendix B the list of observed stars and corresponding measured indices are listed.

2. Calculations

The code for spectrum synthesis is an improved version of that presented in Cayrel et al. (1991), where hydrogen lines are included. LTE is assumed for the synthesis, and for the hydrogen lines a revised version of the code presented in Praderie (1967) was employed.

Abundances are adopted from Grevesse et al. (1996). Oscillator strengths for atomic lines are adopted from Fuhr et al. (1988), Martin et al. (1988) and Wiese et al. (1969) whenever available, otherwise they were obtained by fitting the solar spectrum.

In order to fit the damping constants, it is important to be consistent with the models to be used in the calculation of the grid. In fact atomic constants fitted to the center of the solar disk using the semi-empirical Holweger & Müller (1974, hereafter HM74) solar model atmosphere, showed not to be consistent with calculations for giants, where too large line wings have resulted. A revision of all constants using the integrated solar spectrum (Kurucz et al. 1984) and a solar model atmosphere computed in the same way as those used for the grid was necessary. This is illustrated in Fig. 1a showing the solar spectrum fitted with constants suitable to the HM74 model, but using the present grid of model atmospheres (see Sect. 2.1) for the solar parameters. The wings of the MgI lines are clearly too strong. In Fig. 1b we show the calculation with revised atomic parameters and the solar model of the present grid. It proved to be very important to correct damping constants, given that

Table 1. Comparison of the interaction constant from this work and computed with the collisional broadening theory of Anstee et al. (1997).

Species	$\lambda(\text{\AA})$	χ_{ex} (eV)	$\log gf$	C_6^{present}	C_6^{AOR97}
Mg I	5167.321	2.709	-0.857	0.8E-31	0.29E-30
Mg I	5172.684	2.712	-0.38	0.8E-31	0.29E-30
Mg I	5183.604	2.717	-0.158	0.1E-30	0.29E-30
Fe I	5227.192	1.56	-1.5	0.4E-31	0.29E-31
Fe I	5269.550	0.86	-1.32	0.6E-32	0.18E-31
Fe I	5328.051	0.91	-1.666	0.8E-32	0.19E-31
Fe I	5328.542	1.56	-2.15	0.8E-31	0.28E-31
Fe I	5397.141	0.91	-1.993	0.2E-31	0.19E-31
Fe I	5446.924	0.91	-2.55	0.7E-31	0.19E-31

the discrepancy between calculation and observation becomes increasingly pronounced with the strength of the MgI lines. We have previously computed a grid with atomic parameters derived for the solar spectrum employing the HM74 model, and the indices measured for giants were much stronger than expected.

In order to check our damping constants (and therefore the gf -values, which are determined depending on the adopted damping constant) for FeI and MgI triplet lines, we have computed the damping constants based on the tables of damping constants from the collisional broadening theory of Anstee et al. (1997, hereafter AOR97). For this purpose, we obtained the list of FeI lines from Kurucz (1993), which includes the atomic transitions, available in his CD-ROM 23 and at the web address <http://cfa-www.harvard.edu/amdata/ampdata/kurucz23/sekur.html>. We selected the Fe I lines with solar equivalent widths stronger than $EW(\text{m\AA}) > 200$, and free of blends, as well as the triplet lines of Mg I. We compared our derived interaction constants, as compared to the damping constants derived from Anstee & O'Mara (1995), Barklem & O'Mara (1997) and Barklem et al. (1998). The interaction constant C_6 relates to the damping constant through the formula $\gamma_6/N_H = 17v^{3/5} C_6^{2/5}$ (v is the velocity and N_H is the density of hydrogen atoms). In Table 1 the line parameters and the interaction constants from our fits and those by the AOR97 method are reported for strong lines; the differences are within a factor 3, therefore negligible. For example, this causes a change of about $<0.5\%$ in the Mg₂ index; in order to compensate for this amount, the $\log gf$ value would have to be changed by ≤ 0.12 dex.

The molecular lines of the following molecules were taken into account in the calculations: MgH ($A^2\Pi-X^2\Sigma$), C_2 ($A^3\Pi-X^3\Pi$), CN blue ($B^2\Sigma-X^2\Sigma$), CH ($A^2\Delta-X^2\Pi$), CH ($B^2\Delta-X^2\Pi$), CN red ($A^2\Pi-X^2\Sigma$), TiO α ($C^3\Delta-X^3\Delta$) and TiO γ ($A^3\Phi-X^3\Delta$).

In all cases where possible the Franck-Condon factors with dependence on the rotational quantum number J as given in Dwiwedi et al. (1978) and Bell et al. (1979) were computed and adopted. For vibrational bands for which such values were not available, we adopted a constant value kindly made available to us through computations by P. D. Singh, using the code by Jarman & McCallum (1970).

For the CN blue and CH systems, the line lists by Kurúcz (1993, CD ROM 18) were adopted, where we transformed his tables to our format, recomputing Hönl-London factors using the formulae by Kovács (1969) (a more detailed description is given in Castilho et al. 1999). For the C₂ lines we have carried out a detailed comparison between the Kurúcz line list and the laboratory list by Phillips & Davis (1968). The resulting molecular bands are very similar, so that we have kept the laboratory line list in our calculations.

We have adopted the electronic oscillator strengths $f_{el}(\text{CNred}) = 6.76\text{E-}3$ (Davis et al. 1986; Larsson et al. 1983, Bauschlicher et al. 1988), $f_{el}(\text{CNblue}) = 0.0338$ (Duric et al. 1978), $f_{el}(\text{C}_2) = 0.033$ (Kirby et al. 1979), $f_{el}(\text{CH A}^2\Delta\text{-X}^2\Pi) = 5.257\text{E-}3$ (Brzozowski et al. 1976), and dissociation potentials $D_0(\text{CN}) = 7.65$ eV, $D_0(\text{C}_2) = 6.21$ eV, $D_0(\text{CH}) = 3.46$ eV, $D_0(\text{MgH}) = 1.34$ eV, $D_0(\text{TiO}) = 6.87$ eV (Huber & Herzberg 1979). TiO line lists and constants are described in Schiavon & Barbuy (1999).

2.1. Models

Based on the grid of model atmospheres by Kurúcz (1993), a new grid covering the effective temperature range $4000 \leq T_{\text{eff}} \leq 7000$ K, (in steps of 250 K) using the ATLAS9 code, was computed. The calculations comprise models with α -elements to iron ratios $[\alpha/\text{Fe}] = 0.0$ and $+0.4$.

Three parameters were changed with respect to the original grid, and for this purpose the ATLAS9 code was adapted to a Unix system.

i) The number of layers was increased from 64 to 72. The 8 additional layers represent the outer atmosphere, with optical depths $-6.875 < \log \tau_{\text{Ross}} < -5.875$. These extra layers are important in the formation of the center of strong lines.

ii) The mixing length to pressure scale height ratio $\alpha = \ell/H_p = 0.5$ was adopted, instead of $\alpha = 1.25$ employed in the former models. This value was suggested by Fuhrmann et al. (1993) and Van 't Veer-Menneret & Mégessier (1996) as being more suitable to reproduce the profile of Balmer lines.

iii) No overshooting was considered, given the problems discussed by Van 't Veer-Menneret & Mégessier (1996), Castelli et al. (1997), Castelli (1999) and Heiter et al. (2002).

The convergence of models was imposed to within temperature and flux corrections of $\Delta T < 1$ K, $\Delta\text{Flux} < 1\%$ in the optical depths $-4.875 < \log \tau_{\text{Ross}} < 1.625$ and $\Delta T < 4$ K, $\Delta\text{Flux} < 4\%$ in the higher and lower parts of the atmosphere.

Cooler models were computed in order to have reliability on the fitting functions for T_{eff} around 4000 K, such that the behaviour of curves at 4000 K takes into account a range of points above and below this temperature.

2.2. Grid of synthetic spectra

The grid of stellar synthetic spectra is computed in the wavelength range $\lambda\lambda$ 4600–5600 Å and covers the effective temperatures $4000 \leq T_{\text{eff}} \leq 7000$ K in steps of 250 K, gravities $0.5 \leq \log g \leq 5.0$ in steps of 0.5, and metallicities $[\text{Fe}/\text{H}] = -3.0, -2.5, -2.0, -1.5, -1.0, -0.5, -0.3, -0.2, -0.1,$

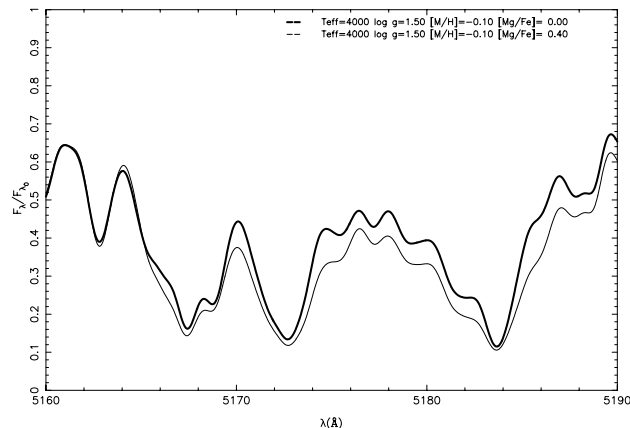


Fig. 2. Spectral region containing the MgI triplet lines computed with $T_{\text{eff}} = 4000$ K, $\log g = 1.5$, $[\text{Fe}/\text{H}] = -0.1$ and $[\alpha/\text{Fe}] = 0.0$ and $+0.4$. The synthetic spectra were convolved with a Gaussian of $FWHM = 1.0$ Å.

0.0 and $+0.3$. Two values of the abundance ratio of α -elements to iron $[\alpha/\text{Fe}] = 0.0$ and $+0.4$ were assumed.

The C and N values which are modified in giants due to convective mixing were adopted to be $[\text{C}/\text{Fe}] = -0.2$ and $[\text{N}/\text{Fe}] = +0.4$ for giants of $\log g \leq 2.0$ and solar for higher gravity stars. The changes in C and N have strong effects in CH and CN bands. The values assumed for microturbulence velocity are $v_t = 1.0$ km s⁻¹ for $\log g \geq 3.0$, $v_t = 1.8$ km s⁻¹ for $1.5 \leq \log g \leq 2.5$, and $v_t = 2.5$ km s⁻¹ for $\log g \leq 1.0$.

Note that the grid was used to estimate atmospheric parameters for different samples of low resolution observed spectra, where errors were found to be of the order of $|T_{\text{eff}}| < 50$ K, $|\log g| < 0.2$, $|[\text{Fe}/\text{H}]| < 0.2$ (Katz 2000a,b, 2001).

In Fig. 2 is given a comparison between synthetic spectra in the MgI triplet lines region, computed with $T_{\text{eff}} = 4000$ K, $\log g = 1.5$, $[\text{Fe}/\text{H}] = -0.1$ and $[\alpha/\text{Fe}] = 0.0$ and $+0.4$.

In Fig. 3 is given the comparison between the observed spectrum of M67: F108 (Table B.1) and the corresponding synthetic spectrum computed with $T_{\text{eff}} = 4360$ K, $\log g = 2.1$, $[\text{Fe}/\text{H}] = -0.36$ and $[\alpha/\text{Fe}] = 0.0$.

3. Indices vs. spectral resolution

The synthetic spectra of the grid were convolved with $FWHM = 2, 3, 3.5, 4, 6, 8$ and 8.3 Å, the latter corresponding to the observations of the Lick group (Worthey & Ottaviani 1997). The Lick indices Fe5270, Fe5335, Mgb and Mg₂, in their early (Burstein et al. 1984; Faber et al. 1985) and revised (Worthey et al. 1994) definitions, were measured on the whole grid of synthetic spectra, for all the convolutions considered. The definitions of the indices are reproduced in Table 2. In this paper we will focus the calculations on the Worthey et al. (1994) definition of the indices.

In Figs. 4a-d the Fe5270, Fe5335, Mgb and Mg₂ indices are plotted as a function of spectral resolution ($FWHM$ in Å). These figures make it clear that the Mgb and Mg₂ indices show essentially no dependence on resolution, showing how robust these indices are.

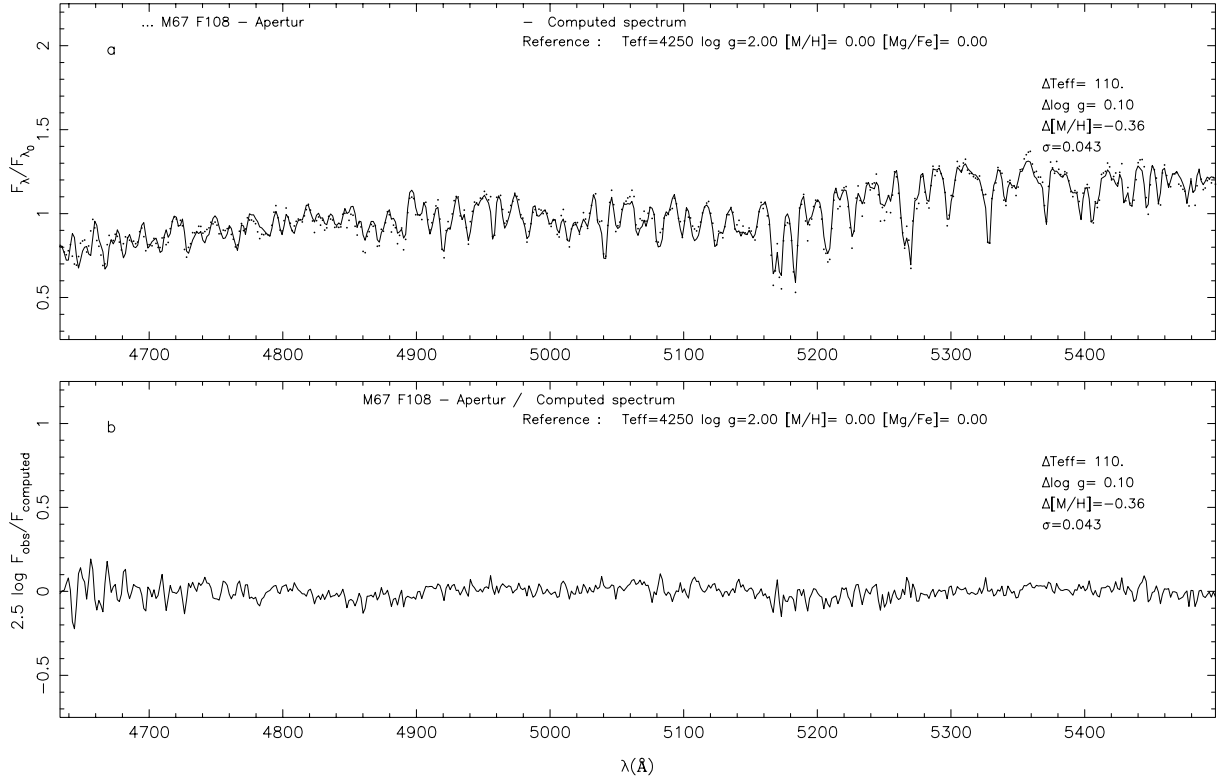


Fig. 3. Comparison of the spectrum of M67: F108 and synthetic spectrum computed with $T_{\text{eff}} = 4360$ K, $\log g = 2.1$, $[\text{Fe}/\text{H}] = -0.36$ and $[\alpha/\text{Fe}] = 0.0$ (upper panel) and residuals (lower panel). The synthetic spectra were convolved with a Gaussian of $FHWM = 3.0$ Å.

Table 2. Definition of indices, where “1984” corresponds to Burstein et al. (1984) and Faber et al. (1985), and “1994” to Worthey et al. (1994).

index name	blue continuum	index bandpass	red continuum
Mg ₂ ¹⁹⁸⁴	4897.00–4958.25	5156.00–5197.25	5303.00–5366.75
Mgb ¹⁹⁸⁴	5144.50–5162.00	5162.00–5193.25	5193.25–5207.00
Fe5270 ¹⁹⁸⁴	5235.50–5249.25	5248.00–5286.75	5288.00–5319.25
Fe5335 ¹⁹⁸⁴	5307.25–5317.25	5314.75–5353.50	5356.00–5364.75
Mg ₂ ¹⁹⁹⁴	4895.125–4957.625	5154.125–5196.625	5301.125–5366.125
Mgb ¹⁹⁹⁴	5142.625–5161.375	5160.125–5192.625	5191.375–5206.375
Fe5270 ¹⁹⁹⁴	5233.150–5248.150	5245.650–5285.650	5285.650–5318.150
Fe5335 ¹⁹⁹⁴	5304.625–5315.875	5312.125–5352.125	5353.375–5363.375

The Fe5270 and Fe5335 indices are weaker for spectra with α -element enhancements than those with $[\alpha\text{-element}/\text{Fe}] = 0.0$. The same effect was present in the calculations by TB95. This is expected, because the α -elements are electron donors (magnesium being the most important in this respect). With α enhancement the electron pressure increases, therefore the continuum absorption by H^- increases. As a consequence, a certain optical depth will be reached at a shallower layer, where the gas pressure is lower, therefore the line wings will be less strong.

The comparison between our calculations and those by TB95 are difficult to establish, given that those authors computed variations of the indices by increasing the abundance of one unique element one by one, whereas in the present work, the calculations were carried out for an enhancement of all α -elements at the same time. The α -elements considered are O, Mg, Si, S, Ca and Ti; Ti nucleosynthesis is in principle associated to the Fe-peak elements (Thielemann et al. 1996), however

the observations strongly suggest a behaviour as an α -element (e.g. Pompéia et al. 2002; François et al. 2003). In addition to that, the measurement of the indices is strongly dependent on the continuum, which is affected in two ways: (i) molecular bands or a number of atomic lines involving the α -elements will affect indices in the pseudo-continuum as well as the features; (ii) the true continuum is dominated by H^- , and therefore it will depend on electron donors, among which the α -elements Mg and Si are important, whereas Ti is not important in this respect. In conclusion, due to the combination of all these effects, it is difficult to make a comparison with the TB95 method of calculation and results.

It is important to note that calculations of α -enhanced spectra is useful for applications in stellar population synthesis in the study of integrated spectra of elliptical galaxies. A discussion on $\langle\text{Fe}\rangle$ and α -element enhancements in ellipticals can be found in e.g. Greggio (1997) and Trager et al. (2000) and

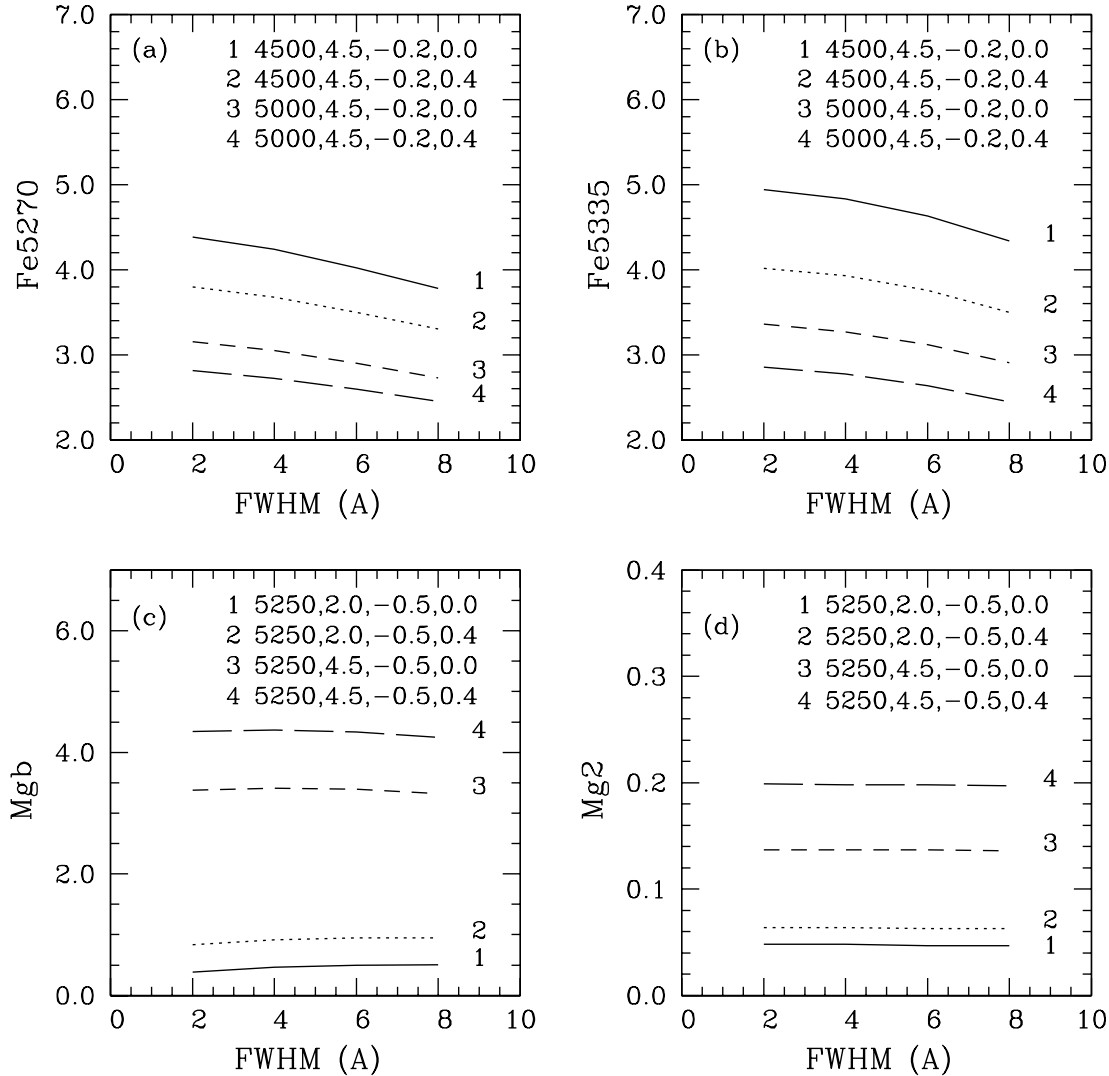


Fig. 4. **a)** Fe5270 and **b)** Fe5335 (as defined by Worthey et al. 1994) vs. $FWHM$ (Å) for dwarfs of $T_{\text{eff}} = 4500$ and 5000 K, $\log g = 4.5$, $[Fe/H] = -0.2$ and $[\alpha/Fe] = 0.0$ and $+0.4$; **c)** Mgb and **d)** Mg₂ vs. $FWHM$ (Å) for a giant and a dwarf of $\log g = 2.0$ and 4.5 , $T_{\text{eff}} = 4500$, $[Fe/H] = -0.5$ and $[\alpha/Fe] = 0.0$ and $+0.4$. See comments in Sect. 3.

references therein. The calculations of TB95 were used by Trager et al. (2000) to infer relations between indices and Fe abundances and the enhancement of a few selected elements.

3.1. Fitting functions

Based on the grid of indices derived for 2660 synthetic spectra with parameters in the range described in Sect. 2.2, we applied the Levenberg-Marquardt method (e.g. Press et al. 1992) to derive functions of the form $\text{index} = [\text{exp}](a + b(\log \theta) + c(\log \theta)^2 + d(\log g) + e(\log g)^2 + f([Fe/H]) + g([Fe/H]^2) + h([\alpha/Fe]) + i(\log \theta)(\log g) + j(\log \theta)([Fe/H]) + k(\log \theta)([\alpha/Fe]) + l(\log \theta)^2(\log g) + m(\log \theta)(\log g)^2)$ (where $\theta = 5040/T_{\text{eff}}$), and [exp] indicates that the index is either the polynomial or the exponential of the polynomial, as indicated in Tables A of the Appendix.

The resulting coefficients for the indices Fe5270, Fe5335 and Mg₂ in their Worthey et al. (1994) definitions are given in

Tables A.1–A.3 for $FWHM = 8.3$ Å, and Tables A.4–A.6 for $FWHM = 3.5$ Å. Each set of fitting functions was divided into four parameter intervals. For the index Mg₂, two of the intervals are not in the exponential form (as indicated in the Tables of Appendix A), in which cases the index is given directly by the polynomial.

It is important to note that since these indices were measured on synthetic spectra, computed in absolute flux, they are not in the Lick System. In order to evaluate the deviation from the Lick system, our fitting functions for $FWHM = 8.3$ Å were applied to the Worthey et al. (1994) sample and compared with the measured indices (as can be seen in Fig. 5 for the index Fe5335). Systematic shifts can be seen, and we interpret them as constants needed to calibrate our theoretical fitting functions to the Lick System. These constants were derived by applying a linear regression to the plots, fixing the slope to 1. The adopted values of $[\alpha/Fe]$ for the Lick sample are described below in Sect. 4.1.

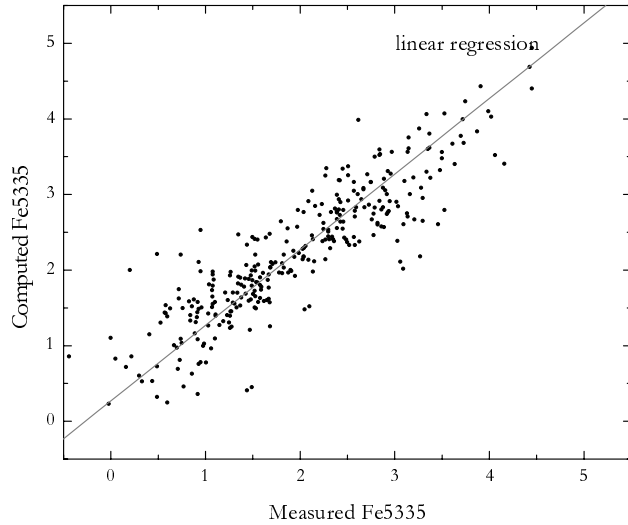


Fig. 5. Comparison of the index Fe5335 between the measured indices of the Worthey et al. (1994) sample and the computed indices from our fitting functions using the stellar parameters provided for that sample. The systematic shift gives the correction that converts the indices derived by the fitting functions to the Lick system.

The same procedure was applied to the fitting functions for $FWHM = 3.5 \text{ \AA}$. In this case, we used our own observations from Table B.3. These observations were flux calibrated, so that we are providing the calibration of the fitting functions for $FWHM = 3.5 \text{ \AA}$ in a flux calibrated system.

The derived calibration constants are provided in Table A.7.

The Mgb index shows a more complicated behaviour, as illustrated in Fig. 6, where $\ln(\text{Mgb})$ vs. $[\text{Fe}/\text{H}]$ is shown for 4 effective temperatures and $\log g = 2.5$. For the cooler stars the behaviour is smooth, whereas for $T_{\text{eff}} > 5250 \text{ K}$ the dependence of the index with metallicity is less smooth; the MgI lines are stronger, but the index is lower, due probably to an enhanced continuum absorption. We preferred not to present a fitting function for this index, since it would involve several functions for limited ranges of parameters. Note that the difficulties in finding fitting functions from the whole grid of synthetic spectra does not appear when using observed indices: Fig. 9 of Schiavon et al. (2002) shows a clear separation between dwarfs and giants, therefore a clear dependence on gravity, and a well behaved function of temperature. The same is obtained with the Mgb indices computed from the synthetic spectra, if we select the same ranges of parameters as shown in Schiavon et al. (2002). More complicated dependences on parameters appear however when the whole space of stellar parameters is used, which is possible with the grid of synthetic spectra.

4. Observations

Low resolution spectra of reference stars were collected as follows:

- 2.2 m telescope of the European Southern Observatory (ESO), with a wavelength resolution of $\Delta\lambda \approx 4.7 \text{ \AA}$, as described in Cayrel et al. (1991);

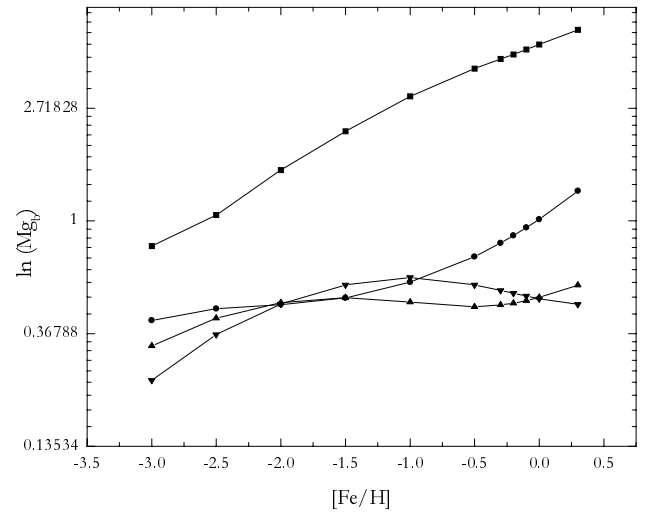


Fig. 6. $\ln(\text{Mgb})$ vs. $[\text{Fe}/\text{H}]$ for $\log g = 2.5$, $[\alpha/\text{Fe}] = 0.0$ and effective temperatures $T_{\text{eff}} = 4250$ (circles), 5250 (triangles), 6000 (downsided triangles) and 6750 K (diamonds). See comments in Sect. 3.1.

- 1.93 m telescope of the Haute Provence Observatory (OHP), with a resolution of $\Delta\lambda \approx 3.0 \text{ \AA}$ as described in Perrin et al. (1995);
- 1.93 m telescope of the OHP, with a resolution of $\Delta\lambda \approx 3.5 \text{ \AA}$ obtained in 1995–1997 with the CARELEC spectrograph (Katz 2000a).

The collected observations for this sample of 97 stars were used to obtain measurements of the indices Fe5270, Fe5335, Mgb and Mg₂ (early and revised definitions). The three sets of observations are given in Appendix B (Tables B.1, B.2 and B.3), together with the measured indices. There are 13 stars in common between Tables B.1 and B.3, which are reported in both tables, given that they were observed in different runs with different resolutions.

4.1. Indices of observed vs. computed spectra

For the comparison of observed and synthetic indices we used the fitting functions for $FWHM = 3.5 \text{ \AA}$.

In order to compare the indices measured on the computed and observed spectra, we assumed the following values of the α -to-iron ratios, based on results from the literature (e.g. McWilliam 1997; Pompéia 2002; Pompéia et al. 2002; François et al. 2003):

- $[\alpha/\text{Fe}] = 0.0$ for stars of $[\text{Fe}/\text{H}] \geq -0.1$
- $[\alpha/\text{Fe}] = 0.1$ for $-0.4 < [\text{Fe}/\text{H}] < -0.1$
- $[\alpha/\text{Fe}] = 0.2$ for $-0.7 < [\text{Fe}/\text{H}] \leq -0.4$
- $[\alpha/\text{Fe}] = 0.3$ for $-0.7 < [\text{Fe}/\text{H}] \leq -1.0$
- $[\alpha/\text{Fe}] = 0.4$ for $[\text{Fe}/\text{H}] < -1.0$,

Fig. 7 gives the computed vs. measured Mg₂ indices for the stars of Tables B.1–B.3, showing a very satisfactory agreement. Due to the stronger dependence of the Fe indices with resolution, the comparisons of the indices Fe5270 and Fe5335 (Figs. 8 and 9) are presented with the observations of Table B.3, which show a very high signal-to-noise ratio (typically of $S/N \approx 300$).

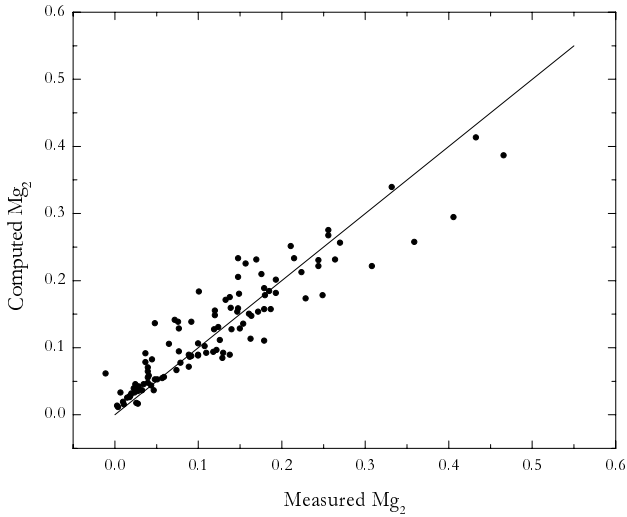


Fig. 7. Computed vs. measured Mg₂ indices for a sample of 97 observed stars listed in Tables B.1–B.3. The solid line is a 1:1 line that would correspond to a perfect match. Standard deviation obtained: 0.006.

As explained in Sect. 3.1, for the Fe5270 and Fe5335, a constant (see Table A.7) must be subtracted from the computed indices since we verify that the computed indices are stronger than the observed ones.

This behaviour of the computed vs. observed Fe features can be partly explained by (a) the calculations are carried out in LTE, therefore the bottom of strong lines are not reproduced, being less deep in the calculations; (b) even in non-LTE, as investigated by McWilliam et al. (1995), the calculation of strong lines are affected by the fact that the model atmospheres do not account correctly for the upper layers and the photosphere/chromosphere boundary; the ATLAS models, which we use here, are more suitable than the MARCS models (e.g. Plez et al. 1992) in this respect, due to a more complete layer coverage. On the other hand, the photosphere/chromosphere boundary would cause a 0.1 dex underestimation of an FeI line of equivalent width larger than 100 mÅ, for a metal-poor giant, according to McWilliam et al. (1995) and the same effect is likely to occur in the present calculations. Note that effects (a) and (b) are interrelated; (c) possible uncertainties in the atomic parameters, given that the Fe indices are composed of several overlapping strong lines, which makes it difficult to detect discrepancies even at very high resolution.

5. Summary

We have computed a grid of synthetic spectra in the wavelength interval $\lambda\lambda$ 4600–5600 Å, for stellar parameters in the range of effective temperatures $4000 \leq T_{\text{eff}} \leq 7000$ K, gravities $0.5 \leq \log g \leq 5.0$, metallicities $[\text{Fe}/\text{H}] = -3.0, -2.5, -2.0, -1.5, -1.0, -0.5, -0.3, -0.2, -0.1, 0.0$ and $+0.3$, and α -elements to iron $[\alpha/\text{Fe}] = 0.0$ and $+0.4$.

The Lick indices Fe5270, Fe5335, Mgb and Mg₂ were measured on the grid of synthetic spectra, and a grid of indices was obtained. Fitting functions for Fe5270, Fe5335 and Mg₂ were

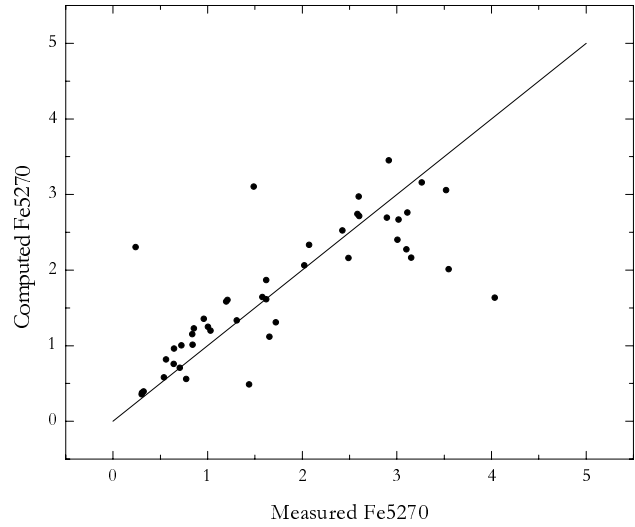


Fig. 8. Computed vs. measured Fe5270 indices for the stars listed in Table B.3. Solid line: same as in Fig. 7. Standard deviation obtained: 0.07.

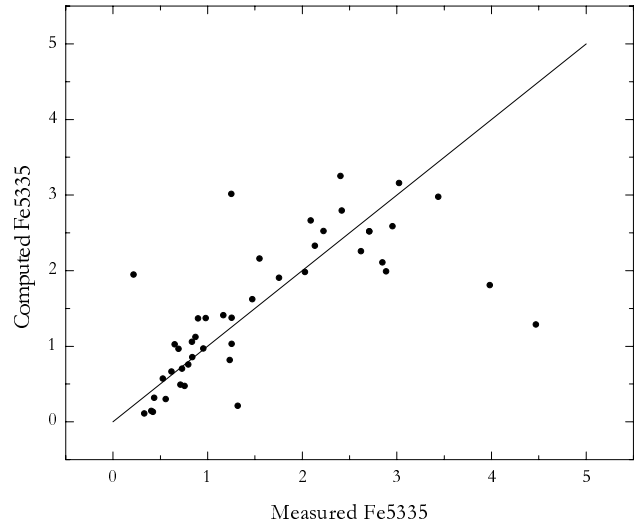


Fig. 9. Computed vs. measured Fe5270 indices for the stars listed in Table B.3. Solid line: same as in Fig. 7. Standard deviation obtained: 0.09.

then derived describing the index value as a function $f(T_{\text{eff}}, \log g, [\text{Fe}/\text{H}], [\alpha/\text{Fe}])$. These relations can be useful for stellar population studies.

A comparison of computed indices to those measured on spectra of reference stars with well-known stellar parameters shows good agreement.

Acknowledgements. We are grateful to the referees A. McWilliam and S. Trager for several important suggestions that considerably improved this paper. BB acknowledges partial financial support from the Observatory of Paris, CNPq/CNRS and Fapesp. PC acknowledges a Fapesp PhD fellowship n° 2000/05237-9.

References

- Alcaíno, G. 1970, ApJ, 159, 325
Alcaíno, G., & Liller, W. 1980, AJ, 85, 1330

- Allard, F., & Hauschildt, P. H. 1995, *ApJ*, 445, 433
- Anstee, S. D., & O'Mara, B. J. 1995, *MNRAS*, 276, 859
- Anstee, S. D., O'Mara, B. J., & Ross, J. E. 1997, *MNRAS*, 284, 202
- Barbuy B. 1994, *ApJ*, 430, 218
- Barklem, P. S., & O'Mara, B. J. 1997, *MNRAS*, 290, 102
- Barklem, P. S., O'Mara, B. J., & Ross, J. E. 1998, *MNRAS*, 296, 1057
- Bauschlicher, C. W., Langhoff, S. R., & Taylor, P. R. 1988, *ApJ*, 332, 531
- Bell, R. A., Dwiwedi, P. H., Branch, D., & Huffaker, J. N. 1979, *ApJS*, 41, 593
- Brzozowski, J., Bunker, P., Elander, N., & Erman, P. 1976, *ApJ*, 207, 414
- Bruzual, A. G., & Charlot, S. 1993, *ApJ*, 405, 538
- Bruzual, A. G., & Charlot, S. 2003, in preparation
- Burstein, D., Faber, S. M., Gaskell, C. M., & Krumm, N. 1984, *ApJ*, 287, 56
- Castelli, F., Gratton, R. G., & Kurucz, R. L. 1997, *A&A*, 318, 841
- Castelli, F. 1999, *A&A*, 346, 564
- Castilho, B. V., Spite, F., Barbuy, B., et al. 1999, *A&A*, 345, 249
- Cayrel, R., Perrin, M.-N., Barbuy, B., & Buser, R. 1991, *A&A*, 247, 108
- Davis, S. P., Shortenhaus, D., Stark, G., et al. 1986, *ApJ*, 303, 892
- Duric, N., Erman, P., & Larsson, M. 1978, *Phys. Scr.*, 18, 39
- Dwiwedi, P. H., Branch, D., Huffaker, J. N., & Bell, R. A. 1978, *ApJS*, 36, 573
- Faber, S. M., Friel, E. D., Burstein, D., & Gaskell, C. M. 1985, *ApJS*, 57, 711
- François, P., Depagne, E., Hill, V., et al. 2003, *A&A*, in press
- Fuhr, J. R., Martin, G. A., & Wiese, W. L. 1988, *Atomic Transition Probabilities: Iron through Nickel*, *J. Phys. Chem. Ref. Data*, 17, Suppl. 4
- Fuhrmann, K., Axer, M., & Gehren, T. 1993, *A&A*, 271, 451
- Gorgas, J., Faber, S. M., Burstein, D., et al. 1993, *ApJS*, 85, 153
- Greggio, L. 1997, *MNRAS*, 285, 151
- Grevesse, N., Noels, A., & Sauval, J. 1996, *ASP Conf. Ser.* 99, ed. S. S. Holt, & G. Sonneborn, 117
- Gulati, R. K., Malagnini, M. L., & Morossi, C. 1993, *ApJ*, 413, 166
- Gunn, J. E., & Stryker, L. L. 1983, *ApJS*, 52, 121
- Heiter, U., & Kupka, F., van 't Veer-Menneret, C., et al. 2002, *A&A*, 392, 619
- Holweger, H., & Müller, E. 1974, *Sol. Phys.*, 39, 19 (HM74)
- Huber, K. P., & Herzberg, G. 1979, *Constants of Diatomic Molecules, van Nostrand Reinhold, New York Spectra of Diatomic Molecules* (Am. Elsevier Pub. Co.)
- Jarmain, W. R., & McCallum, J. C. 1970, *TRAPRB* (London, Ontario, Dept. Phys., Univ. Western Ontario)
- Jacoby, G. H., Hunter, G. A., & Christian, C. A. 1984, *ApJ*, 419, 592
- Katz, D. 2000a, Ph.D. Thesis, Université de Paris VII
- Katz, D. 2000b, *Aussois School on Physique et modelisation des atmospheres stellaires*, ed. J.P. Zahn, C. Catala, 97
- Katz, D. 2001, *First COROT/MONS/MOST Ground Support Workshop*, ed. C. Sterken (Vrije Universiteit Brussel), 67
- Kirby, K., Saxon, R. P., & Liu, B. 1979, *ApJ*, 231, 637
- Kovács, I. 1979, *Rotational Structure in the Spectra of Diatomic Molecules* (Am. Elsevier Pub. Co.)
- Kurucz, R. L. 1993, *CD-ROM* 13, 14, 18, 23
- Kurucz, R. L., Furenlid, I., & Brault, J. 1984, *Solar flux atlas from 296 to 1300 nm*, National Solar Observatory Atlas, Sunspot, New Mexico: National Solar Observatory
- Larsson, M., Siegbahn, P. E. M., & Ågren, H. 1983, *ApJ*, 272, 368
- Lee, S.-W. 1977, *A&AS*, 27, 381
- Lejeune, Th., Cuisinier, F., & Buser, R. 1997, *A&AS*, 125, 229
- Lejeune, Th., Cuisinier, F., & Buser, R. 1998, *A&AS*, 130, 65
- Martin, G. A., Fuhr, J. R., & Wiese, W. L. 1988, *Atomic Transition Probabilities: Scandium through Manganese*, *J. Phys. Chem. Ref. Data*, 17, Suppl. 3
- McWilliam, A. 1997, *ARA&A*, 35, 503
- McWilliam, A., Preston, G. W., Sneden, C., & Searle, L. 1995, *AJ*, 109, 2757
- Montgomery, K. A., Marschall, L. A., & Janes, K. A. 1993, *AJ*, 106, 181
- Perrin, M.-N., Friel, E. D., & Bienaymé, O., et al. 1995, *A&A*, 298, 107
- Phillips, J. G., & Davis, S. P. 1968, *The Swan System of the C₂ molecule* (U. of California Press)
- Plez, B., Brett, J. M., & Nordlund, Å. 1992, *A&A*, 256, 551
- Pompéia, L. 2002, Ph.D. Thesis, U. São Paulo
- Pompéia, L., Barbuy, B., & Grenon, M. 2002, *ApJ*, 566, 845
- Praderie, F. 1967, *Ann. Astrophys.*, 30, 31
- Press, W. H., Teukolsky, S. A., Vetterling, W. T., & Flannery, B. P. 1992, *Numerical Recipes* (Cambridge Univ. Press)
- Schiavon, R. P., & Barbuy, B. 1999, *ApJ*, 510, 934
- Schiavon, R. P., Faber, S. M., Castilho, B. V., & Rose, J. A. 2002, *ApJ*, 580, 850
- Soubiran, C., Katz, D., & Cayrel, R. 1998, *A&AS*, 133, 221
- Thielemann, F.-K., Nomoto, K., & Hashimoto, M. 1996, *ApJ*, 460, 408
- Trager, S. C., Worthey, G., Faber, S. M., Burstein, D., & González, J. J. 1998, *ApJS*, 116, 1
- Trager, S. C., Faber, S. M., Worthey, G., & González, J. J. 2000, *AJ*, 119, 1645
- Tripicco, M. J., & Bell, R. A. 1995, *AJ*, 110, 3035
- van 't Veer-Menneret, C., & Mégessier, C. 1996, *A&A*, 309, 879
- Wiese, W. L., Martin, G. A., & Fuhr, J. R. 1969, *Atomic Transition Probabilities: Sodium through Calcium*, *J. Phys. Chem. Ref. Data*, NSRDS-NBS-22
- Worthey, G. 1994, *ApJS*, 95, 107
- Worthey, G., Faber S. M., González, J. J., & Burstein, D. 1994, *ApJS*, 94, 687
- Worthey, G., & Ottaviani, D. L. 1997, *ApJS*, 111, 377